Optics Communications 331 (2014) 128–132

Contents lists available at ScienceDirect

Optics Communications

journal homepage: www.elsevier.com/locate/optcom

Strong light-matter coupling in plasmonic microcavities

Lijian Zhang, Fuchun Xi, Jie Xu, Qinbai Qian, Peng Gou, Zhenghua An *

Laboratory of Advanced Materials, State Key Laboratory of Surface Physics and Key Laboratory of Micro and Nano Photonic Structures (Ministry of Education), Fudan University, Shanghai 200433, China

ARTICLE INFO

Article history:
Received 11 May 2014
Accepted 30 May 2014
Available online 12 June 2014

Keywords:
Strong coupling
Plasmonic microcavity
Intersubband transitions
Propagating surface plasmons
Localized surface plasmons
Polaritons

ABSTRACT

We numerically study the strong coupling between quantum well (QW) intersubband transitions (ISBT) and the plasmonic resonance of metal-dielectric-metal (MDM) microcavities. In this system, the lowest-order energy state of plasmonic resonance is a hybrid mode of propagating surface plasmons (PSP) and localized surface plasmons (LSP). For a given lowest-order resonance, the mode transformation can be realized between PSP mode and LSP mode by varying the plasmonic microcavity structure, which opens a new freedom to modulate the coupling interaction of light and matter. With the cavity mode transforming from LSP mode to PSP mode, the coupling strength increases from 20.75% to 25.75%, which is mainly dominated by the polarization conversion ratio $\langle E_z^2\rangle/\langle E^2\rangle$ of plasmonic modes.

1. Introduction

The strong coupling phenomenon of light-matter interaction is studied initially in the atomic physics [1,2] and still attracting tremendous research interest. The physical regime has been investigated in diverse systems, such as ultracold atoms in optical cavities [3], Cooper-pair boxes [4], excitons in semiconductor QWs microcavities [5] and ISBT of doped QWs in microcavites [6,7]. Among these systems, intersubband microcavites have become the hot spot of research on light-matter interaction, owing to its unique potential as a powerful tool to investigate cavity electrodynamics [8,9] and to the successful applications of ISBT in a number of optoelectronic devices like quantum well infrared photodetectors (QWIPs) [10] and quantum cascade lasers (QCLs) [10,12].

In intersubband microcavity, when an intersubband transition is resonant with a cavity mode and the rate of a photon exchanged between them is faster than the damping rates of light and matter fields, the strong coupling will happen. In this regime, the normal modes of the system are called cavity polaritons and they exhibit an anticrossing behavior in energy with a splitting $2\hbar\Omega_R$, where Ω_R is called the vacuum Rabi frequency. To date, some efforts have been devoted to intersubband polaritons in infrared with wavelength-scale planar optical cavities [7,11,13]. Due to QWs only sensitive to the electric-field component aligned along the growth direction (usually labeled as z component), high incidence angles are required when these structures are illuminated by TM wave. As a result, systems that can couple to normal incident light with a non-negligible E_z component are highly desired.

More recently, the monolayer metamaterials [14,15] and MDM microcavities with sub-wavelength confinement of the mode such as patch antennas [6,16] and LC resonators [17] have been used to demonstrate intersubband polaritons. These systems can not only provide strong field enhancement but also couple light at normal incidence. However, optical modes in such microcavities are hardly to be tuned because each system can only support a single type cavity mode. In this letter, we design a MDM plasmonic microcavity with the top gold film perforated with cross-hole arrays which can couple vertically incident radiation at high efficiency. The lowest-order resonance of the plasmonic microcavity is a hybridized mode of PSP mode and LSP mode [18] other than a single type cavity mode [6,16]. We study the strong coupling in the plasmonic microcavities embedded with doped semiconductor QWs and manage to tune the coupling strength by transforming the plasmonic modes in microcavities.

2. Structure and simulation method

As shown in Fig. 1(a), we study a sandwiched plamonic microcavity, which consists of a top Au film perforated with an array of cross-shaped holes, a bottom continuous Au film, and a GaAs/AlGaAs QWs layer. The cross-hole array has a period of P, length of L, and width of W with $W=0.2L$ fixed. The gold layer thickness is fixed at $t=0.1\ \mu m$ and the dielectric constant of Au is given by a standard Drude model [19] with the following parameters: $\varepsilon_\infty=1$, $\omega_p=1.365\times10^{16}$ rad/s, and $\gamma_{Au}=5.78\times10^{13}$ Hz.

* Corresponding author.
E-mail address: anzhenghua@fudan.edu.cn (Z. An).

http://dx.doi.org/10.1016/j.optcom.2014.05.066
0030-4018/

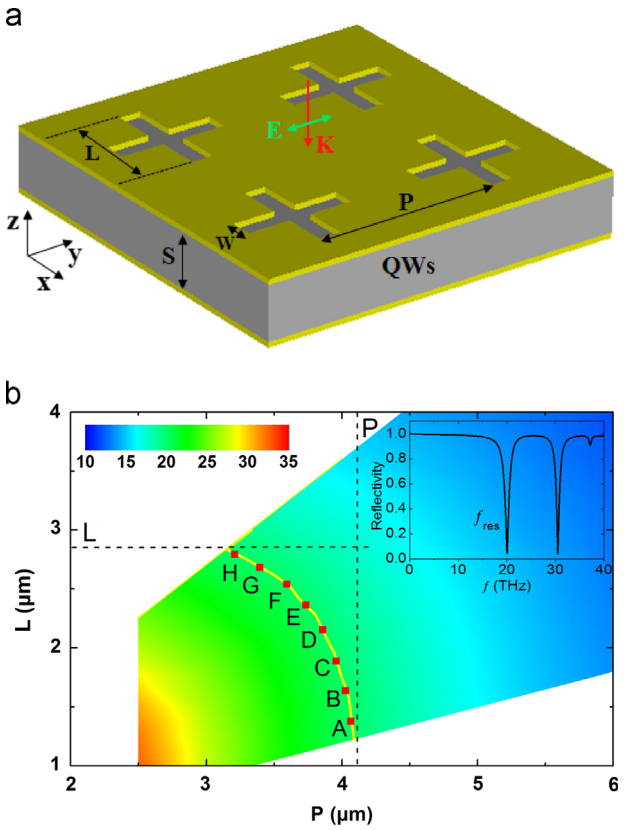

Fig. 1. (a) Schematic view of Au/QWs/Au plasmonic microcavity embedded with quantum wells. The structure is illuminated by light polarized along the y axis at normal incidence. (b) Color contour plot of the lowest-order resonance frequency f_{res} as a function of P and L for the studied plasmonic microcavity, with yellow solid curve depicting the case with $f_{res}=20$ THz. The inset shows the reflection spectrum of H microcavity. (For interpretation of the references to color in this figure legend, the reader is referred to the web version of this article.)

Since interactions among resonance modes are complicated with the variation of S [20], the thickness of microcavity is fixed at $S=1$ μm. Such a sub-wavelength microcavity can provide not only a strong field enhancement in cavity but also better light confinement than conventional dielectric cavities, leading to a high resonance Q-factor. In our simulations, the Lorenzian model is applied to depict the permittivity of semiconductor QWs [7]:

$$\varepsilon_z(f)=\varepsilon_{GaAs}+\frac{N_s e^2 f_{osc}}{4\pi^2 m_0 \varepsilon_0 L_{eff}}\frac{1}{(f_{QW}^2-f^2)-i\gamma f} \tag{1}$$

in which N_s is the electronic sheet density in QW, e is the electronic charge, m_0 is the electronic rest mass, ε_0 is the vacuum permittivity, L_{eff} is the effective QW width, $f_{osc}=(4\pi m_0/\hbar)f_{QW}d^2$ is the ISBT oscillator strength of QWs, and d is the dipole matrix element between the envelope function of two subbands,which is set as 2 nm here. f_{QW} is the central frequency of the ISBT and γ is the intersubband linewidth. We set $\varepsilon_x=\varepsilon_y=\varepsilon_{GaAs}$ since QWs are only sensitive to the E_z component of the electromagnetic field due to the polarization selection rule. Based on the typical experimental conditions, we set $N_s=1\times10^{12}$ cm^{-2}, $L_{eff}=10$ nm, and $\gamma=0.05$. Numerical simulation is performed by the finite-difference time-domain (FDTD) method [21]. The structure is illuminated by plane wave with the E-field polarized along the y axis at normal incidence.

3. Results and discussion

We begin with the case the QWs are fully depleted ($N_S=0$) and the spacer becomes dispersiveless, i.e., $\varepsilon_{GaAs}=12.9$. Resonant modes of different origins in this case have been studied systematically in our previous publication [20]. Due to the continuous Au film on the back, our systems do not allow light transmission, and therefore, we only focus on its reflection properties in the following. Fig. 1(b) shows the contour plot of the lowest-order resonance f_{res} versus the array period P and cross-hole length L. We note that f_{res} is a decreasing function of P and L, and therefore, to obtain a given frequency f_{res}, P must increase when L decreases and vice versa. The yellow solid curve is the equal-frequency line of $f_{res}=20$ THz. As $L\to0$ (i.e., very small hole size), f_{res} becomes insensitive to the hole size and depends solely on the array period. In this limiting case, the resonance is dominated by the periodicity-induced surface plasmons (PSP) [22]. On the other hand, as $L\to P$ (i.e., large hole size), the resonance f_{res} is contributed mainly by the fundamental localized surface plasmons (LSP) of cross holes [23,24]. In order to ease the following discussion, we pick out eight points (A,B,C,D,E,F,G,H) from the solid curve in Fig. 1(b), with the A-struture defining the small hole limit (with PSP-like mode) while the H-cavity defining the large hole limit (with LSP-like mode). From A to H, the plasmonic mode changes from PSP-like mode to LSP-like mode. In the inset, the reflection spectrum of H microcavity is plotted with the lowest-order resonance $f_{res}=20$ THz.

To understand the differences between PSP mode and LSP mode, the electric field distribution of A and H at 20 THz in yz plane at $x\approx0$ are displayed in Fig. 2(a) and (b) when the phase is corresponding to the strongest electric field. Fig. 2(a) and 2(b) correspond to the field distribution of PSP mode and LSP mode respectively. We note that the two modes have different distributions along the z-direction and different electric field polarizations. The PSP mode is mostly confined in the sandwiched region while the LSP mode localizes around the cross holes, partly in the cavity and partly in the air. Due to QWs only sensitive to E_z component, Fig. 2(c) and 2(d) depicts the computed distribution of $|E_z|^2$ of A and H in xy-plane at $z\approx-0.1$ μm. The E_z field is mainly concentrated in the hole center in case Fig. 2(d), the signatures of the LSP mode. On the other hand, in Fig. 2(c), the E_z field forms a strip-like distribution along the x direction, indicating the formation of a PSP mode propagating along the y direction.

Taking into account the plasmonic microcavity used for enhancing the interaction of light and ISBT, we quantitatively study the average field enhancement over the cavity volume in A–H cases. The enhancement factors can be calculated by the following two equations:

$$\frac{\langle E^2\rangle}{\langle E_0^2\rangle}=\int\frac{|E^2|\,dx\,dy\,dz}{|E_0^2|P^2S} \tag{2}$$

and

$$\frac{\langle E_z^2\rangle}{\langle E_0^2\rangle}=\int\frac{|E_z^2|\,dx\,dy\,dz}{|E_0^2|P^2S} \tag{3}$$

where integration is performed over one unit cell volume and E_0, E, E_z represent the incident field, the cavity field and the z-component of cavity field respectively. The value of $\langle E_z^2\rangle/\langle E_0^2\rangle$ represents the ability of the device to absorb light waves. As shown in Fig. 3, when the structure changes from A to H, the enhancement factor$\langle E^2\rangle/\langle E_0^2\rangle$ (red curve) and $\langle E_z^2\rangle/\langle E_0^2\rangle$ (blue curve) increase firstly and then decrease, but the gap between the two curves gradually increase. It suggests that the ratio of the normal incident light converted from TE to TM polarization is different for PSP mode and LSP mode. The maximum enhancement is achieved for F structure with $\langle E^2\rangle/\langle E_0^2\rangle\approx4.8$ and $\langle E_z^2\rangle/\langle E_0^2\rangle\approx4$, in which the trapped photons and the damped photons reach equilibrium [23]. Therefore, F structure design is more suitable for photo-detection. If we compare the result with the case without any plasmonic coupler, we will find